Research Square

Preprints are preliminary reports that have not undergone peer review.
They should not be considered conclusive, used to inform clinical practice,
or referenced by the media as validated information.

Neuromuscular Control During Tai Chi in Individuals With Knee Osteoarthritis: Broadly Preserved Muscle Synergy Architecture With Selective Alterationsin Functional Recruitment

Meijin Hou
Fujian University of Traditional Chinese Medicine
Xiangbin Wang
Fujian University of Traditional Chinese Medicine
Shengxing Fu
The Second Affiliated Hospital and Yuying Children's Hospital of Wenzhou Medical University
Dongwei Liu
Zhejiang University of Finance and Economics
Chenyi Guo
Tsinghua University
Ye Ma
maye@nbu.edu.cn
Ningbo University

Article

Keywords: muscle synergy; non-negative matrix factorization; surface electromyography; knee osteoarthritis; Tai Chi; motor control

Posted Date: November 5th, 2026

DOI: https://doi.org/10.21203/rs.3.rs-10586009/v1

License: This work is licensed under a Creative Commons Attribution 4.0 International License.
Read Full License

Additional Declarations: No competing interests reported.

Title page

Neuromuscular Control During Tai Chi in Individuals With Knee Osteoarthritis: Broadly Preserved Muscle Synergy Architecture With Selective Alterations in Functional Recruitment

Running title: Preserved synergy architecture and selective recruitment alterations

Article type: Research

Authors
Meijin Hou[1,2] (ORCID: 0000-0003-4830-5615), Xiangbin Wang[1,2] (ORCID: 0000-0002-1293-8755), Shengxing Fu[3] (ORCID: 0000-0001-8983-6653), Dongwei Liu[4,*] (ORCID: 0000-0002-0697-0548), Chenyi Guo[5] (ORCID: 0000-0002-8222-5179), Ye Ma[6,*] (ORCID: 0000-0002-1964-045X)

Affiliations
[1] National and Local Joint Engineering Research Centre of Rehabilitation Medical Technology, Fujian University of Traditional Chinese Medicine, No.1 West Qiuyang Road, Fuzhou, 350122, China
[2] College of Rehabilitation Medicine, Fujian University of Traditional Chinese Medicine, No.1 West Qiuyang Road, Fuzhou, 350122, China
[3] Department of Physical Medicine and Rehabilitation, The Second Affiliated Hospital and Yuying Children's Hospital of Wenzhou Medical University, Wenzhou, China
[4] School of Information Technology and Artificial Intelligence, Zhejiang University of Finance and Economics, No.18 Xueyuan Road, Hangzhou, 310018, China
[5] Department of Electronic Engineering, Tsinghua University, No.100 Xueyuan Road, Beijing, 100084, China
[6] Research Academy of Grand Health, Faculty of Sports Sciences, Ningbo University, 818 Fenghua Road, Ningbo, 315211, China

Corresponding authors
Dongwei Liu
School of Information Technology and Artificial Intelligence, Zhejiang University of Finance and Economics
No.18 Xueyuan Road, Hangzhou, 310018, China
Email: dongwei.liu@zufe.edu.cn

Ye Ma
Research Academy of Grand Health, Faculty of Sports Sciences, Ningbo University
818 Fenghua Road, Ningbo, 315211, China
Email: maye@nbu.edu.cn

Contributing author emails
Meijin Hou: meijinhou@fjtcm.edu.cn; Xiangbin Wang: wangxbin@fjtcm.edu.cn; Shengxing Fu: fushengxing1996@163.com; Chenyi Guo: guochy@mail.tsinghua.edu.cn

Keywords: muscle synergy; non-negative matrix factorization; surface electromyography; knee osteoarthritis; Tai Chi; motor control

Manuscript contents
Figures: 9 | Tables: 6 | References: 42 | Supplementary files: 2

Neuromuscular Control During Tai Chi in Individuals With Knee Osteoarthritis: Broadly Preserved Muscle Synergy Architecture With Selective Alterations in Functional Recruitment

Abstract

Background: Although Tai Chi is widely recommended for knee osteoarthritis (KOA), its muscle-level control, group differences and the movements that best reveal them remain unclear. Using muscle synergies extracted by non-negative matrix factorization (NMF), we identified Tai Chi's key lower-limb muscles, tested whether synergy architecture or recruitment differed between groups and ranked movements for assessment research.

Methods: Bilateral surface EMG from 16 lower-limb muscles was recorded in 69 participants (52 KOA and 17 healthy controls) during eight-form Tai Chi (17 movement-by-side conditions). Synergies were extracted by shared-basis consensus NMF and evaluated using five measures: synergy number, muscle weights, whole-vector similarity, functional contribution (each muscle's share of reconstructed EMG), and activation profiles (cluster-based permutation testing). Contribution compositions were centred-log-ratio transformed and compared using studentised permutation tests with global Benjamini–Hochberg correction. Other statistical tests used predefined within-family adjustments for multiple comparisons. The measures formed a descriptive composite index for ranking movements.

Results: Reconstructed EMG contribution was dominated by the quadriceps (≈49%), assisted by hip and posterior-chain muscles, forming six bilaterally symmetric synergy modules. Synergy architecture showed limited KOA–HC differences: synergy number, overall similarity and muscle weights differed minimally. Differences concentrated in recruitment rather than structure: 11/272 contribution contrasts survived global correction, with KOA showing higher gluteus medius contribution in two conditions and controls higher contribution from the tibialis anterior, vastus medialis, biceps femoris, medial gastrocnemius and rectus femoris in selected conditions. Activation profiles differed in 26/99 synergies (34 cluster-corrected windows, 24 KOA-higher), most numerous in Repulse Monkey but longest in Cloud Hands. The integrated index ranked Heel Kick and Repulse Monkey as most KOA-divergent, which the activation-profile measure alone would have missed.

Conclusions: Tai Chi recruits a compact set of key lower-limb muscles organised into six bilaterally paired synergy modules whose architecture was broadly similar between groups. KOA was associated with selective, movement-specific differences in relative contribution and activation profiles within these largely shared synergies. No single measure captured every affected movement, so a descriptive integrated index ranked candidates. These muscles and movements are candidates for task-specific motor-control training and compact KOA assessment batteries, warranting prospective evaluation.

Keywords: muscle synergy; non-negative matrix factorization; surface electromyography; knee osteoarthritis; Tai Chi; motor control

1 Background

Knee osteoarthritis (KOA) is a leading cause of joint pain and functional disability [1, 2], and exercise therapy is regarded as a first-line, non-pharmacological treatment [2]. Tai Chi—a traditional mind–body exercise characterised by slow continuous movements, sustained weight-bearing, multi-joint coordination and a semi-squat, flexed-knee stance—has been shown to reduce pain, and improve balance and physical function in people with KOA [3]. Tai Chi has therefore been recommended in clinical guidelines for KOA management by the American College of Rheumatology (ACR) [4] and the Osteoarthritis Research Society International (OARSI) [5].

Tai Chi tradition describes this ideal movement quality as "relaxed strength"; in biomechanical terms, this can be examined as coordinated, phase-dependent recruitment of lower-limb muscles during force generation [6]. Whether it also entails lower antagonist co-contraction remains uncertain, because reported associations have depended on the gait task and study design [7]. For individuals with KOA, the motor control challenges of Tai Chi are compounded by the disease's characteristic muscle impairments, including weakness and altered co-activation patterns [8–10]. Tai Chi has also been noted to be "beneficial, with few risks" for patients with KOA [2]. Therefore, understanding how Tai Chi is controlled at the muscle level and how that control differs in KOA would benefit both the mechanistic understanding of this exercise and the design of safer and more effective rehabilitation protocols.

Muscle synergies offer a framework suited to characterising such multi-muscle control. Because the musculoskeletal system carries many more muscles than a task has mechanical degrees of freedom, the central nervous system is thought to simplify control by recruiting a small number of co-activation modules—muscle synergies—rather than commanding each muscle independently [11]. A synergy has two parts that can be examined separately: a mostly fixed spatial structure (which muscles form a module and their relative weights within it) and a time-varying activation profile (how strongly and when the module is recruited). Synergies are recovered from surface electromyography by matrix decomposition, of which non-negative matrix factorization (NMF) is by far the most widely used: it yields parts-based, non-negative decompositions [12] and is widely used to summarise EMG as candidate muscle-coordination modules [13], whereas linear alternatives (principal- and independent-component analysis) and, more recently, non-linear autoencoders have also been proposed [14]. Crucially, a synergy's two aspects can change independently, and which one a condition affects is mechanistically informative: studies of human balance show that *spatially fixed* synergies are flexibly *retimed* by task-level feedback—the nervous system regulating centre-of-mass kinematics through synergy recruitment—to meet changing demands across the phases of a movement without altering their architecture [15]. The slow, continuously shifting weight transfer of Tai Chi is precisely such a feedback-regulated postural task, making muscle synergies a natural lens on how its multi-joint coordination is organised.

In neurological injury, development or training, by contrast, synergy architecture can reorganise, merging or fractionating into different muscle groupings [16, 17]. Such reorganisation is plausible in KOA, which is accompanied by knee-extensor and

broader muscle impairments, including hip weakness, as well as altered vasti and lower-limb co-activation patterns during gait [8–10]. Whether a condition such as KOA remodels the synergy structure, or instead is associated only with how a broadly similar structure is used—in relative muscle contribution or activation profile—is therefore an open and clinically meaningful question, one that requires the two facets to be measured separately and across the whole routine.

A small body of work has begun to examine Tai Chi at the neuromuscular level. Using NMF, Zhang et al. characterised the muscle synergies of a single Tai Chi action—the leg-stirrup kick—in twelve elite young athletes, identifying four synergy patterns within each phase and a phase-specific optimal pattern for lift, extension and recovery. Recruitment of the selected patterns correlated with centre-of-gravity velocity, which the authors interpreted as an indicator of dynamic stability [6]. At the level of co-activation, long-term Tai Chi practitioners showed lower ankle-antagonist co-contraction than Tai Chi-naïve older adults during dual-task, but not single-task, gait; a six-month randomised comparison found no difference between Tai Chi and usual care [7]. Together these studies show that muscle synergies and co-activation can be quantified in Tai Chi-related tasks, while leaving the effects of training on co-contraction unresolved.

This prior work, however, has looked at only one movement, and only in small groups of young, elite practitioners. Three questions therefore remain open. First, the muscle synergies of the complete Tai Chi routine—which muscles contribute most to its reconstructed EMG, and how they group into modules—have not been described across all its movements. Second, it is not known whether KOA changes these synergies by reorganising their structure, or only by changing how they are recruited. Third, it is unclear whether any such change is spread evenly across the routine or concentrated in a few movements—a question with direct practical value, since knowing which movement best exposes the disorder would help clinicians assess and monitor it. One practical obstacle has made these questions hard to answer: because NMF returns synergies in an arbitrary order and scale, synergies extracted independently for each person cannot be compared directly across subjects or groups. Existing studies handle this in several ways—comparing independently extracted synergies across subjects by pairwise similarity and cross-reconstruction [18], matching independently extracted synergy sets by similarity [19], or extracting a single basis from the concatenated data of the whole sample [20] —but all share one requirement: the synergies must first be brought onto a common reference before groups can be compared.

Our study addresses these gaps. To overcome the comparison obstacle, we developed a hybrid shared-reference procedure that combines the pooled-basis rationale of concatenated NMF [20] with a multi-start consensus strategy adapted from Brunet et al. [21]. For each condition, we extracted a consensus basis from the pooled KOA and HC data and matched each participant's independently extracted synergies to that reference. This provides a common reference ordering for group comparison. We then decomposed the group comparison into five complementary measures that deliberately separate synergy *architecture* (number, overall similarity, muscle weights) from synergy *recruitment* (functional contribution and activation profiles). Applying this framework to every movement of the routine, and integrating the five measures into a

single index, further allows the movements themselves to be ranked by how strongly they expose KOA-related change, identifying candidate assessment tasks.

The study addressed three questions: (1) Which lower-limb muscles are the key contributors during Tai Chi? (2) Is KOA associated with differences in synergy architecture, relative muscle contribution or activation profiles? (3) Which movements show the greatest KOA–HC neuromuscular differences and therefore warrant prospective evaluation as candidate assessment tasks? To answer them, we identify the key muscles, separate architectural from recruitment changes, and combine all five measures into an integrated index that nominates specific movements as candidate, hypothesis-generating assessment tasks.

2 Methods

2.1 Participants

Sixty-nine participants were studied: 52 with KOA and 17 healthy controls (HC). A diagnosis of KOA was established by senior clinicians in line with the Chinese guidelines for the diagnosis and treatment of osteoarthritis [22]. The study protocol, informed-consent form and participant-recruitment materials were approved by the Ethics Review Committee of the Rehabilitation Hospital Affiliated to Fujian University of Traditional Chinese Medicine (approval no. 2024KY-038-01). All methods were performed in accordance with the principles of the Declaration of Helsinki and with applicable institutional guidelines and regulations. All participants provided written informed consent before participation. To be eligible, patients required clinically and radiographically confirmed knee disease, and both single-knee and both-knee presentations were accepted. Candidates were not enrolled if they reported pain in any other lower-limb joint or in the lower back, carried a diagnosis of rheumatoid arthritis or of any neurological or musculoskeletal disorder, or had any further condition likely to compromise lower-limb function. Their baseline characteristics, including body-mass index (BMI), symptom duration and Kellgren–Lawrence (KL) radiographic grade, are summarised in Table 1; the groups did not differ significantly in sex, age, height, weight or BMI (all $p > 0.12$); the full participant-level baseline data are provided in Additional file 1: Table S1.

2.2 Tai Chi routine and EMG recording

Each participant performed a standardised simplified eight-form Tai Chi routine [23], comprising 10 named movements, listed here in routine order by English name (Pinyin-initial code, Pinyin): Opening Form (QS, qǐ shì), Repulse Monkey (DJG, dào juǎn gōng), Brush Knee and Twist Step (LXAB, lōu xī ǎo bù), Part the Wild Horse's Mane (YMFZ, yě mǎ fēn zōng), Cloud Hands (YS, yún shǒu), Golden Rooster Stands on One Leg (JJDL, jīn jī dú lì), Heel Kick (DJ, dēng jiǎo), Grasp the Sparrow's Tail (LQW, lǎn què wěi), Cross Hands (SZS, shí zì shǒu) and Closing Form (SS, shōu shì), also shown in Fig. 1; throughout this paper the English movement names are used in narrative text, while the Pinyin-initial codes (DJ, DJG, ...) are retained as compact labels in figures, tables, data files, and exact movement–side condition names. Surface

Table 1 Baseline characteristics of the participants and between-group comparison. Values are mean (SD) for continuous variables unless otherwise stated.

Characteristic	KOA ($n = 52$)	HC ($n = 17$)	p
Sex, women/men	39/13	9/8	0.13^{f}
Age (years)	62.1 (6.0)	62.8 (6.5)	0.73^{t}
Height (m)	1.61 (0.07)	1.63 (0.07)	0.15^{u}
Weight (kg)	62.1 (10.2)	60.9 (9.2)	0.64^{t}
BMI (kg/m^2)	23.8 (2.6)	22.8 (2.7)	0.18^{t}
Symptom duration (months)†	66 (36–120)	NA	—
KL grade, 1/2/3	3/33/16	NA	—

KOA, knee osteoarthritis; HC, healthy controls; BMI, body-mass index; KL, Kellgren–Lawrence radiographic grade; IQR, interquartile range; NA, not applicable (HC have no KOA-specific clinical measures). — in the p column indicates that no between-group test was performed because the clinical measure was not applicable to HC. †Disease duration was not normally distributed and is given as median (IQR). Between-group test (superscript on each p value): ^{t}Welch's t-test (age, weight, BMI; both groups normal by Shapiro–Wilk); ^{u}Mann–Whitney U test (height; KOA non-normal); ^{f}Fisher's exact test (sex). The full participant-level baseline data underlying these summaries are given in Additional file 1: Table S1.

electromyography (sEMG) was recorded bilaterally from 16 lower-limb muscles, eight per side. The recorded muscles were gluteus medius (GMd), gluteus maximus (GMx), rectus femoris (RF), vastus lateralis (VL), vastus medialis (VM), biceps femoris (BF), tibialis anterior (TA) and medial gastrocnemius (MG). Electrodes were positioned over each muscle following the SENIAM recommendations [24]. sEMG signals were converted into linear envelopes (band-pass 20–450 Hz, full-wave rectification, low-pass envelope at 20 Hz) sampled at 2000 Hz. Bilateral movements were analysed separately according to the stance (support) leg, yielding 17 movement×side analysis conditions; the three unilateral forms (Opening Form, Cross Hands, and Closing Form) contributed a single condition each.

2.3 Signal preprocessing

Each trial's 16-channel envelope was time-normalised by cubic-spline interpolation onto a common, movement-specific number of samples N, so that all trials of the same movement became length-matched. For each movement, N was set to its median trial duration multiplied by a target rate of 20 Hz and rounded to the nearest 5 samples; this held the effective temporal resolution at ≈20 Hz across movements of differing duration. Amplitudes were then normalised within participant and muscle: each channel was divided by that participant's peak value across all of their trials, so weights and activations are dimensionless and comparable across participants. The result for each trial is a non-negative matrix $V \in \mathbb{R}^{16\times N}$. Trials were grouped into the 17 analysis conditions for synergy extraction.

2.4 Muscle-synergy extraction

Muscle synergies were modelled by non-negative matrix factorization (NMF) as

$$V \approx WH, \tag{1}$$

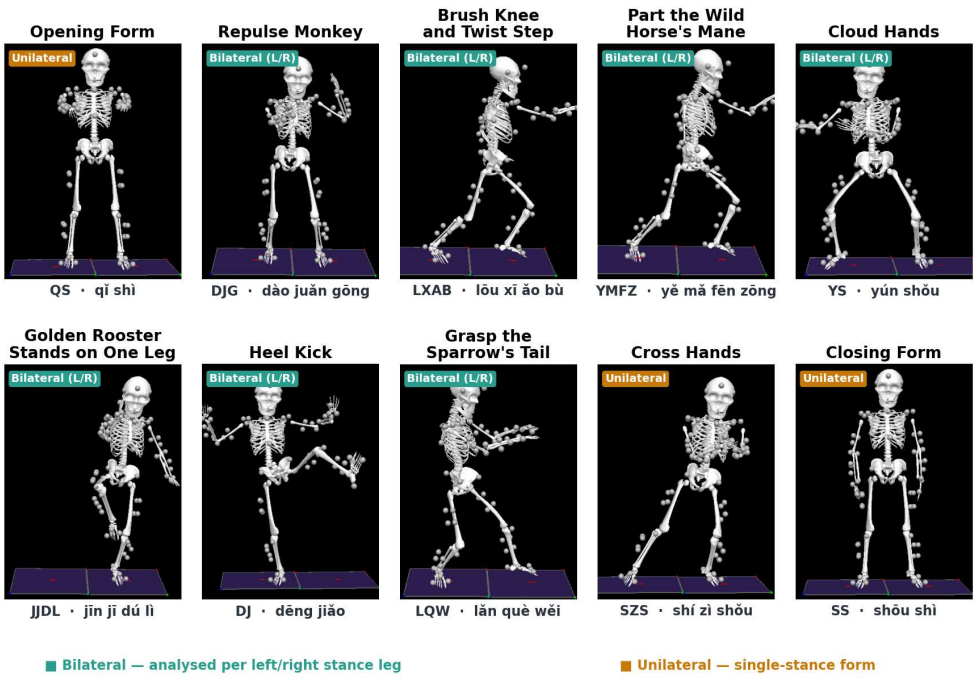


Fig. 1 The ten Tai Chi movements analysed. Each panel shows the movement with, beneath it, the English name (used in narrative text), the Pinyin-initial code (used in figures, tables, data files, and exact condition names) and the Pinyin. In routine order, these are Opening Form (QS), Repulse Monkey (DJG), Brush Knee and Twist Step (LXAB), Part the Wild Horse's Mane (YMFZ), Cloud Hands (YS), Golden Rooster Stands on One Leg (JJDL), Heel Kick (DJ), Grasp the Sparrow's Tail (LQW), Cross Hands (SZS) and Closing Form (SS). The seven bilateral movements (DJG, LXAB, YMFZ, YS, JJDL, DJ, LQW) are analysed separately by stance (support) leg, giving left/right (L/R) conditions, whereas the three unilateral forms (QS, SZS, SS) contribute a single condition each, for 17 movement×side analysis conditions in total.

where V is the non-negative muscle×time matrix (trials concatenated along time), $W \in \mathbb{R}^{16\times k}$ holds the k muscle-weight vectors and $H \in \mathbb{R}^{k\times\cdot}$ the time-varying activation coefficients. All factorisations used scikit-learn's NMF with the Frobenius-norm objective, coordinate-descent solver, maximum 500 iterations and tolerance 10^{-4}.

Shared reference basis. For each condition, we estimated a shared muscle-weight reference basis W_{shared} from all trials pooled across KOA and HC participants, following the pooled-basis rationale of concatenated NMF [20]. To improve stability, we used a multi-start consensus strategy adapted from Brunet et al. [21]: one deterministic NNDSVD initialisation [25] and 49 random restarts. Our adaptation clustered the L2-normalised columns of W from all 50 factorisations into k groups using k-means and used the resulting centroids as the columns of W_{shared}. This basis defined the canonical synergy reference labels for that condition; participant- and trial-level synergies remained independently estimated and were matched to the reference as described below.

Rank selection. Following standard NMF muscle-synergy practice, the rank k was selected from the reconstruction-quality curve rather than fixed a priori [13, 16]. Global reconstruction quality was quantified using an R^2-style variance accounted for: $\mathrm{VAF} = 1 - \|V - WH\|_F^2 / \|V - \bar{V}\|_F^2$, where $\bar{V}$ is the grand mean of V. The primary criterion was the smallest k with global VAF ≥ 0.90, a commonly used reconstruction-quality criterion in synergy analyses [16]. If no tested rank reached this threshold, we used a pre-specified elbow fallback: the smallest k for which adding the next synergy increased VAF by $< 5\%$ [16]. VAF and cophenetic-stability diagnostics were estimated on up to 8000 randomly subsampled time columns for computational tractability; final NMF extraction at the selected rank used the full pooled matrix.

Subject- and trial-level synergies. For each participant and, separately, for each trial, an independent NMF was fitted at the rank selected for that condition (NNDSVD initialisation). Its weight columns were L2-normalised to resolve scale and then matched to W_{shared} by the Hungarian algorithm (maximising column-wise cosine similarity), thereby standardising their order and labels across participants. Reconstruction VAF and recruitment were retained for each shared, subject-level, and trial-level solution.

Global all-movements basis. For the descriptive global-basis analysis (Fig. 2), we extracted a single consensus-NMF basis from data pooled across all 17 movement×side conditions. Before pooling, each condition was capped at 3500 time columns by stratified random subsampling so that longer movements or conditions with more trials did not dominate the global basis. The global rank ($k = 6$) was selected using the same VAF/elbow rule.

2.5 Five comparison measures

KOA and HC were compared using five complementary measures; the common statistical conventions are given in Section 2.7.

1. **Synergy number.** Within each movement×side condition, the optimal rank was determined separately for each participant (same VAF≥0.90/elbow rule applied to that participant's trials), and the per-participant counts were compared between groups across the 17 conditions. For the seven bilateral movements, stance-leg (left/right) and group effects on synergy number were tested jointly with a two-way mixed permutation ANOVA per movement, with side as the within-participant factor and group as the between-participant factor. Because synergy number is a small non-normal integer, inference used permutation rather than the F distribution: the side main effect was tested by permuting side labels within each participant, and the group main effect and side×group interaction by permuting group labels of whole participants (1000 permutations each; BH-FDR across the seven movements, per effect). The interaction term tests whether any stance-leg asymmetry is disease-specific. Follow-up left–right comparisons within each group used two-sided Wilcoxon signed-rank tests with BH-FDR correction across the seven bilateral movements within each group.

2. **Synergy similarity.** Because module-by-module comparison requires the two group bases to have the same rank, KOA-only and HC-only bases were independently re-extracted at a common rank $k_{\text{compare}} = \max(k_{\text{KOA}}, k_{\text{HC}})$ for each condition, where k_{KOA} and k_{HC} are the group-specific selected ranks from the synergy-number analysis. This choice avoids truncating the group with the larger selected rank. The resulting bases were Hungarian-matched by cosine similarity, and each matched pair was scored by the cosine of its unit weight vectors ($\cos = a \cdot b / \|a\| \|b\|$); a pair with $\cos \geq 0.80$ was classified as similar under the prespecified threshold. Inter-individual variability was assessed by extracting a pooled KOA+HC reference basis at the same common rank, aligning each participant's free-fit weights to it, and comparing the resulting per-participant cosine-to-reference between groups.
3. **Muscle weights.** Using subject-level W matrices aligned to the shared basis, each muscle weight—one $W_{m,k}$ entry per (condition, synergy, muscle)—was compared between groups (1584 weights in total: $16 \times \sum_{\text{conditions}} k_{\text{condition}} = 16 \times 99$).
4. **Functional contribution.** To estimate each muscle's share of reconstructed EMG activity (combining structural weight with realised recruitment), the contribution of muscle m was defined, per participant and condition, as

$$C_m = \sum_k W_{m,k} \int H_k(t)\, dt, \tag{2}$$

the integral of the reconstructed envelope attributable to muscle m, normalised within participant to a percentage of the summed reconstructed EMG envelope ($\sum_m C_m = 100\%$). Because these 16 percentages form a composition, they were transformed before inference using the centred log-ratio (CLR) transformation [26],

$$[\text{clr}(\mathbf{C})]_m = \log\left(\frac{C_m}{g(\mathbf{C})}\right), \qquad g(\mathbf{C}) = \left(\prod_{j=1}^{16} C_j\right)^{1/16}, \tag{3}$$

where $g(\mathbf{C})$ is the geometric mean of the 16 strictly positive contribution components for that participant and condition. For each condition and muscle, KOA and HC CLR values were compared with a two-sided studentised permutation test using the Welch statistic and 9999 group-label permutations [27]. Raw percentages were retained for descriptive reporting. Averaged across participants (per condition, and pooled across conditions for the overall ranking), the same percentages give the key-muscle profile.
5. **Activation profiles.** For each synergy and condition, each participant's mean activation curve (averaged over trials) was formed over the normalised cycle, and the two groups' curves compared with a one-dimensional cluster-based permutation test. A Welch's t statistic (unequal-variance pointwise comparison) was computed at each time point. Contiguous points exceeding the two-sided $\alpha = 0.05$ Student-t critical value with $\text{df} = \min(n_{\text{KOA}}, n_{\text{HC}}) - 1$—a deliberately conservative cluster-forming threshold—formed candidate clusters, each summarised by its

mass (summed t); inference rests on the permutation null below rather than on this threshold. Each observed cluster mass was tested against the null distribution of the maximum absolute cluster mass over 1000 label permutations (fixed seed), giving a cluster-corrected p. Each significant window was further described by its duration (% cycle), direction (higher activation in KOA or HC), and mean cluster t statistic (cluster mass divided by the number of time points). As a complementary per-participant view, the location of each synergy's peak activation (% of cycle)— a periodic variable, with 0% ≡ 100%— was compared between groups with a permutation test on the circular mean direction: for each group the mean angle $\bar{\theta} = \mathrm{atan2}(\sum_i \sin\theta_i, \sum_i \cos\theta_i)$, with $\theta = 2\pi\, p/100$ and p the peak location (% of cycle), was computed. The absolute wrapped angular difference $|\Delta\bar{\theta}|$ between groups was tested against its null from 1000 group-label permutations (fixed seed), with Benjamini–Hochberg FDR applied across the 99 testable condition– synergy pairs (≥ 5 participants per group).

2.6 A synthesis synergy index based on five comparison measures

To rank movements descriptively, we combined the five measures into a *composite synergy index* developed for this study. Each measure first contributed one continuous, per-condition summary metric, derived from the comparisons in Section 2.5 and oriented so that larger values denote greater KOA–HC divergence: (D1) the absolute group-comparison effect size of the synergy-number difference; (D2) structural divergence, 1− the mean matched-synergy cosine; (D3) the mean absolute group-comparison effect size for muscle weights; (D4) the mean absolute group-comparison effect size for contribution; and (D5) the total duration of cluster-corrected activation-profile differences. D1 and D3 use the Cohen's d or rank-biserial r effect-size metrics defined in the statistical analysis section below. D4 uses Hedges' g on the CLR-transformed contributions. Absolute values were used so that larger values consistently indicate greater group separation. Collect these as $x_{d,c}$ for measure $d \in \{1, \ldots, 5\}$ and analysis condition $c \in \{1, \ldots, 17\}$. Because the five metrics are on different scales, each was standardised across the 17 conditions,

$$z_{d,c} = \frac{x_{d,c} - \mu_d}{\sigma_d}, \tag{4}$$

where μ_d and σ_d are the mean and population standard deviation of metric d over the conditions; $z_{d,c}$ is thus dimensionless and expressed in standard-deviation units relative to the average movement. The composite synergy index of condition c is the equal-weighted mean of the five standardised metrics,

$$S_c = \frac{1}{5} \sum_{d=1}^{5} z_{d,c}. \tag{5}$$

By construction S_c is dimensionless and centred near zero across conditions ($S_c > 0$ indicating a more KOA-divergent movement than average); it is a *relative* ranking

with no absolute scale, no units and no built-in significance threshold. As a sensitivity analysis, a recruitment-weighted variant using only the two altered measures (the mean of $z_{4,c}$ and $z_{5,c}$) was also computed.

2.7 Statistical analysis

All between-group analyses used the participant as the unit of analysis. For synergy-number and muscle-weight comparisons, normality was assessed separately in each group using the Shapiro–Wilk test. When both groups were approximately normal, values are reported as mean (SD) and compared using Welch's t-test with Cohen's d; otherwise, values are reported as median (IQR) and compared using the two-sided Mann–Whitney U test with rank-biserial r [28]. Analysis outputs retained the test statistic, p and FDR-adjusted p values, and signed effect size; Welch comparisons also retained the Satterthwaite degrees of freedom for muscle weights. Under the implemented Mann–Whitney orientation, $r > 0$ indicates higher values in HC and $r < 0$ indicates higher values in KOA.

Functional-contribution comparisons instead used the single prespecified CLR studentised-permutation procedure described above. For each muscle×condition comparison, let $\bar{z}_{\mathrm{K}}$, s_{K} and n_{K} denote the mean, standard deviation and sample size of the KOA CLR values, with the corresponding HC quantities denoted by subscript H. Hedges' g was calculated as [29]

$$
\begin{aligned}
s_p &= \sqrt{\frac{(n_{\mathrm{K}}-1)s_{\mathrm{K}}^2 + (n_{\mathrm{H}}-1)s_{\mathrm{H}}^2}{n_{\mathrm{K}}+n_{\mathrm{H}}-2}}, \\
J &= 1 - \frac{3}{4(n_{\mathrm{K}}+n_{\mathrm{H}})-9}, \\
g &= J\,\frac{\bar{z}_{\mathrm{K}} - \bar{z}_{\mathrm{H}}}{s_p}.
\end{aligned}
\tag{6}
$$

Thus, positive values indicate higher relative contribution in KOA. For each of $B = 2000$ bootstrap replicates, participants were sampled with replacement separately within the two groups and g was recalculated. The pointwise percentile-bootstrap confidence interval was

$$
\mathrm{CI}_{95\%} = \left[Q_{0.025}\left(\{g_b^*\}_{b=1}^{B}\right), Q_{0.975}\left(\{g_b^*\}_{b=1}^{B}\right) \right], \tag{7}
$$

where Q_p denotes the empirical p-quantile of the bootstrap estimates[30]. These confidence intervals were not multiplicity-adjusted; multiplicity control was applied to the permutation p values through BH-FDR.

Effect-size magnitudes were interpreted descriptively using conventional benchmarks [31]: $|d|$ or $|g|$ of approximately 0.2, 0.5 and 0.8, and $|r|$ of approximately 0.1, 0.3 and 0.5, indicate small, medium and large effects, respectively.

Benjamini–Hochberg FDR correction was applied across the 17 conditions for synergy number and across the 16 muscles within each condition– synergy combination for muscle weights (99 separate families). Thus, muscle-weight adjustment was

local to each condition– synergy family rather than global across all 1584 weights. For functional contribution, the primary family comprised all 272 muscle×condition comparisons; separate 16-muscle condition-wise adjustments were retained as an exploratory sensitivity analysis. Activation-profile inference used maximum-cluster-mass correction within each condition–synergy profile, with no additional correction across the 99 profiles. Peak-timing comparisons used the across-profile BH-FDR correction described above.

Analyses used all participants with a complete 16-muscle composition for the relevant condition, without imputation; available-case sample sizes ranged from 41 to 52 KOA and 12 to 17 HC participants. Cluster-based permutation provided an empirical null distribution and cluster-level multiplicity control without relying on random-field-theory inference, which was not used given the small control samples ($n_{\mathrm{HC}} = 12$–17).

2.8 Software and reproducibility

Analyses were performed in Python 3.14.4 using NumPy 2.4.6, SciPy 1.17.1, pandas 3.0.3, scikit-learn 1.9.0 (NMF with the coordinate-descent solver and k-means) and Matplotlib 3.10.9; baseline Excel input used openpyxl 3.1.5, and DOCX report exports used python-docx 1.2.0. Primary NMF fits used deterministic NNDSVD initialisation. All remaining stochastic operations—random NMF restarts, k-means consensus clustering, column subsampling, and permutation tests—used fixed seeds; subject- or movement-specific seeds were derived from SHA-256 hashes rather than Python's process-dependent `hash()` function. Supporting data and results are supplied in two supplementary files. Additional file 1 provides participant-level baseline data, detailed condition-level results, methodological information and the complete set of supplementary figures. `Supplementary_Tables.xlsx` provides the machine-readable per-condition statistics underlying the reported comparisons.

3 Results

3.1 Global synergy modules are bilaterally symmetric

Pooling all movements, lower-limb neuromuscular control reduced to six bilaterally symmetric synergy modules (Fig. 2): left/right knee-extension synergies (quadriceps-dominated), left/right hip–posterior-chain synergies (gluteal/hamstring/gastrocnemius-dominated) and left/right ankle-dorsiflexion synergies (tibialis-anterior-dominated). Reconstruction accuracy was nearly identical between groups (VAF: KOA 0.69, HC 0.70), indicating that the global synergy basis was shared by KOA and healthy controls.

3.2 Synergy number is stable between groups but asymmetric across stance legs

Synergy number did not differ between groups (4/17 conditions at raw $p < 0.05$; 0/17 after FDR; Fig. 3). The four uncorrected differences were movement-specific: KOA

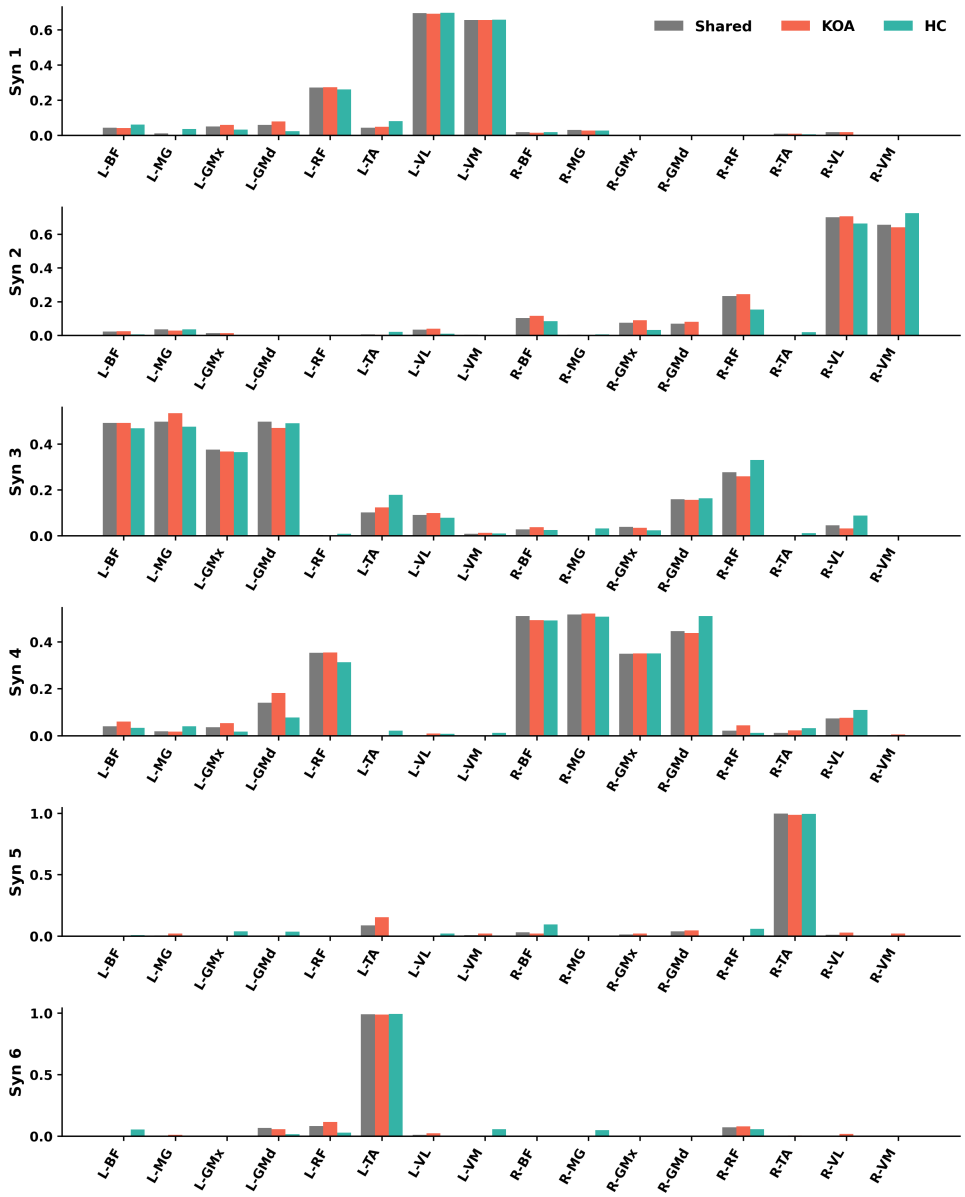


Fig. 2 Global muscle-synergy basis extracted after pooling all movements (rank $k = 6$). Weight distributions are shown for the shared basis and for each group (Shared/KOA/HC). The synergy modules are arranged in bilaterally symmetric pairs, and the weights are highly concordant between groups. Abbreviations: KOA, knee osteoarthritis; HC, healthy controls; BF, biceps femoris; MG, medial gastrocnemius; GMx, gluteus maximus; GMd, gluteus medius; RF, rectus femoris; TA, tibialis anterior; VL, vastus lateralis; VM, vastus medialis; L/R prefixes denote left/right side.

selected higher ranks in Heel Kick (DJ-L: KOA median 8.0 vs HC 7.0, raw $p = 0.011$, BH-FDR-adjusted $p = 0.093$; DJ-R: KOA 8.0 vs HC 6.5, raw $p = 0.027$, adjusted $p = 0.115$) and Golden Rooster Stands on One Leg (JJDL-R: KOA 7.0 vs HC 6.0, raw $p = 0.017$, adjusted $p = 0.096$), whereas HC required more synergies in Repulse Monkey (DJG-R: HC 5.0 vs KOA 4.0, raw $p = 0.008$, adjusted $p = 0.093$). These trends clustered in dynamic single-limb or backward-stepping actions.

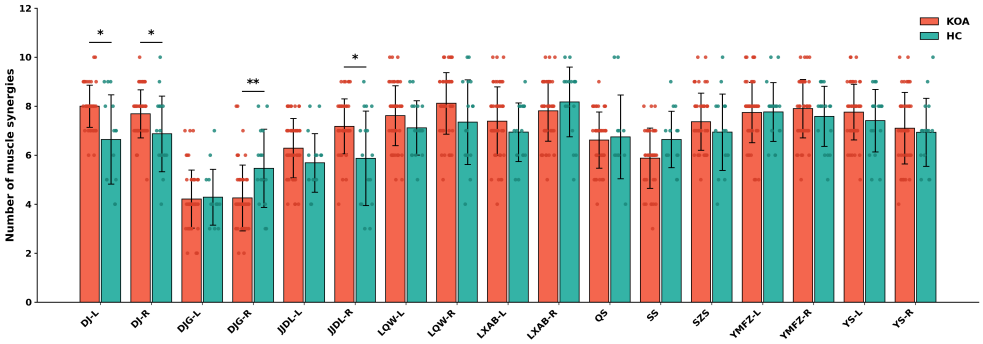


Fig. 3 Number of synergies per Tai Chi movement, KOA versus HC (bars show mean, error bars SD, dots individual values; connecting lines indicate raw $p < 0.05$). No analysis condition reached significance after FDR correction. Abbreviations: KOA, knee osteoarthritis; HC, healthy controls; SD, standard deviation; FDR, false discovery rate; QS, Opening Form; DJG, Repulse Monkey; LXAB, Brush Knee and Twist Step; YMFZ, Part the Wild Horse's Mane; YS, Cloud Hands; JJDL, Golden Rooster Stands on One Leg; DJ, Heel Kick; LQW, Grasp the Sparrow's Tail; SZS, Cross Hands; SS, Closing Form; L/R, left/right stance leg; NA, single-stance movement.

Although there are no significant differences in synergy number between the two groups on the per-side comparison, a joint two-way (side×group) analysis revealed a stance-leg asymmetry that was mostly shared rather than disease-specific (Table 2). The side main effect was significant after FDR in four of seven bilateral movements: Golden Rooster Stands on One Leg, Grasp the Sparrow's Tail, Brush Knee and Twist Step, and Cloud Hands. Thus, the two stance legs recruited different numbers of synergies. The direction was not uniform: the right leg used more synergies in Golden Rooster Stands on One Leg, Grasp the Sparrow's Tail, and Brush Knee and Twist Step, whereas the left leg used more in Cloud Hands. Crucially, the side×group interaction, which tests whether this asymmetry differs between KOA and healthy controls, was significant for only one movement, Repulse Monkey (BH-FDR-adjusted $p = 0.007$): follow-up paired comparisons showed a higher synergy number during right than left stance in HC (BH-FDR-adjusted $p = 0.034$), but no side difference in KOA (BH-FDR-adjusted $p = 0.972$). For the other six movements, no interaction survived FDR correction, so their stance-side patterns were not shown to differ between groups. The group main effect reached significance for Heel Kick and Golden Rooster Stands on One Leg when averaged across stance sides.

Table 2 Two-way mixed ANOVA of synergy number per bilateral movement (side within participant, group between participants; permutation inference, 1000 permutations; Benjamini–Hochberg FDR across the seven movements, per effect). The descriptive statistic in each k_L and k_R column follows the cell-specific Shapiro–Wilk result: mean (SD) for approximately normal cells and median (IQR) otherwise; entries shown as ranges are medians (IQRs). F_s, F_g, $F_{s\times g}$: side, group and interaction F-statistics with BH-FDR-adjusted p values (bold = significant at adjusted $p < 0.05$). k_L, k_R: synergy number on the left/right stance leg, by group.

Movement	k_L^{K}	k_R^{K}	k_L^{H}	k_R^{H}	F_s ($p_{\mathrm{FDR},s}$)	F_g ($p_{\mathrm{FDR},g}$)	$F_{s\times g}$ ($p_{\mathrm{FDR},s\times g}$)
JJDL	6.5 (5.0–7.0)	7.0 (7.0–8.0)	5.0 (5.0–6.0)	6.0 (1.9)	14.40 (**0.003**)	10.49 (**0.010**)	0.95 (0.497)
LQW	8.0 (7.0–8.0)	8.0 (7.0–9.0)	7.1 (1.1)	7.4 (1.7)	16.15 (**0.002**)	3.34 (0.143)	1.26 (0.484)
LXAB	7.0 (6.5–8.0)	8.0 (7.0–9.0)	6.9 (1.2)	9.0 (8.0–9.0)	13.05 (**0.002**)	0.00 (1.000)	5.26 (0.115)
YS	8.0 (7.0–9.0)	7.0 (6.0–8.0)	8.0 (6.8–8.0)	6.9 (1.4)	12.90 (**0.002**)	0.90 (0.540)	0.58 (0.568)
DJG	4.0 (4.0–5.0)	4.0 (3.0–5.0)	4.0 (4.0–5.0)	5.5 (1.7)	3.46 (0.101)	5.74 (0.051)	14.29 (**0.007**)
DJ	8.0 (8.0–8.0)	8.0 (7.0–8.0)	6.6 (1.8)	6.6 (1.3)	3.04 (0.101)	18.49 (**0.007**)	0.39 (0.567)
YMFZ	8.0 (7.0–8.0)	8.0 (7.0–9.0)	8.0 (7.0–8.0)	8.0 (7.0–8.0)	0.38 (0.518)	0.28 (0.776)	1.14 (0.484)

Abbreviations: KOA, knee osteoarthritis; HC, healthy controls; ANOVA, analysis of variance; FDR, false discovery rate; IQR, interquartile range; K, KOA; H, HC; SD, standard deviation; QS, Opening Form; DJG, Repulse Monkey; LXAB, Brush Knee and Twist Step; YMFZ, Part the Wild Horse's Mane; YS, Cloud Hands; JJDL, Golden Rooster Stands on One Leg; DJ, Heel Kick; LQW, Grasp the Sparrow's Tail; SZS, Cross Hands; SS, Closing Form; L/R, left/right stance leg; NA, single-stance movement.

3.3 Synergy similarity remains high between KOA and controls

Synergy similarity was largely consistent: the cosine similarity between each matched KOA–HC synergy pair had a median of 0.95 (IQR 0.81–0.98), and 95/125 matched synergies (76%) exceeded the prespecified cosine similarity threshold (≥ 0.80) (Fig. 4). Most of these sub-threshold pairs were higher-order synergies beyond the shared rank rather than failed matches of the dominant modules. Repulse Monkey showed the lowest similarity of any movement.

Beyond the group-mean comparison, each participant's synergies were also compared with a pooled reference: the median cosine-to-reference was 0.89 in both groups, and the per-subject values did not differ between KOA and HC for any synergy (0/125 after FDR), indicating that KOA neither shifted the average synergy pattern nor widened its spread across individuals.

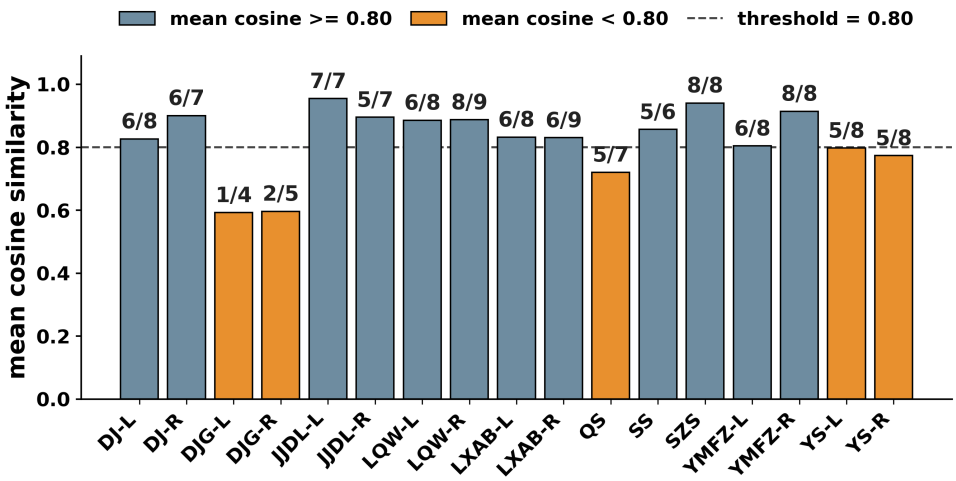


Fig. 4 Synergy similarity (cosine) of matched weight vectors between KOA and HC for each movement. Bars show the mean cosine similarity across matched synergy pairs within each movement–side condition; blue bars have mean cosine ≥ 0.80 and orange bars have mean cosine < 0.80. The dashed line marks the prespecified similarity threshold (0.80), and labels above bars show the number of synergies above the threshold over the total number of matched synergies. Most synergy pairs reach the similarity threshold; DJG is the most notable exception. Abbreviations: KOA, knee osteoarthritis; HC, healthy controls; QS, Opening Form; DJG, Repulse Monkey; LXAB, Brush Knee and Twist Step; YMFZ, Part the Wild Horse's Mane; YS, Cloud Hands; JJDL, Golden Rooster Stands on One Leg; DJ, Heel Kick; LQW, Grasp the Sparrow's Tail; SZS, Cross Hands; SS, Closing Form; L/R, left/right stance leg; NA, single-stance movement.

3.4 Muscle weights show only sparse group differences

The per-muscle weight comparison likewise showed sparse group differences in architecture: only 25/1584 weights (1.6%) differed between groups after FDR correction. Notably, these few differences were not randomly distributed but were concentrated in a small set of muscles, mainly the gluteals (gluteus maximus, 7 weights; gluteus medius, 2), rectus femoris (5), medial gastrocnemius (3), biceps femoris (3), and vastus medialis (3), and occurred in the same movements highlighted by the recruitment analyses, with Heel Kick and Golden Rooster Stands on One Leg accounting for 12/25. The few weight differences that survived correction therefore involved largely the same muscles that show functional-contribution differences below, rather than a separate set: hip stabilisers, rectus femoris, and gastrocnemius (all higher in KOA), and vastus medialis (higher in HC).

Table 3 Muscle synergy weights that differed between groups after FDR correction (25/1584). All rows used Mann–Whitney U; values are median (IQR). Effect size is signed rank-biserial r; $|r|$ gives the magnitude, and Direction indicates the group with the higher weight.

Cond.	Syn	Muscle	KOA	HC	r	p_{FDR}	Direction
DJ-L	5	L BF	0.26 (0.14–0.39)	0.07 (0.01–0.21)	-0.49	0.031	KOA↑
DJ-L	5	L MG	0.39 (0.17–0.50)	0.05 (0.00–0.27)	-0.55	0.030	KOA↑
DJ-L	5	L GMx	0.33 (0.12–0.49)	0.13 (0.03–0.19)	-0.49	0.031	KOA↑
DJ-R	5	L RF	0.14 (0.09–0.18)	0.04 (0.02–0.07)	-0.51	0.019	KOA↑
DJ-R	5	R BF	0.39 (0.14–0.62)	0.09 (0.02–0.24)	-0.53	0.019	KOA↑
DJ-R	5	R MG	0.41 (0.14–0.58)	0.09 (0.01–0.28)	-0.47	0.025	KOA↑
DJG-L	8	L VM	0.00 (0.00–0.00)	0.01 (0.00–0.10)	0.57	0.005	HC↑
DJG-R	9	L GMx	0.08 (0.01–0.64)	0.01 (0.00–0.02)	-0.55	0.023	KOA↑
JJDL-L	3	L BF	0.74 (0.07–0.93)	0.95 (0.84–0.98)	0.52	0.015	HC↑
JJDL-L	3	L RF	0.07 (0.04–0.14)	0.02 (0.00–0.05)	-0.53	0.015	KOA↑
JJDL-L	3	R GMx	0.02 (0.01–0.04)	0.00 (0.00–0.01)	-0.45	0.037	KOA↑
JJDL-L	4	L VM	0.00 (0.00–0.06)	0.11 (0.05–0.29)	0.62	0.002	HC↑
JJDL-L	4	R RF	0.21 (0.02–0.47)	0.03 (0.00–0.08)	-0.46	0.041	KOA↑
JJDL-R	2	L GMx	0.18 (0.09–0.33)	0.07 (0.02–0.11)	-0.50	0.043	KOA↑
LQW-L	1	L GMx	0.04 (0.02–0.06)	0.02 (0.01–0.04)	-0.44	0.027	KOA↑
LQW-L	1	L RF	0.03 (0.01–0.07)	0.00 (0.00–0.02)	-0.51	0.013	KOA↑
LQW-L	1	R GMx	0.04 (0.02–0.09)	0.01 (0.00–0.03)	-0.59	0.004	KOA↑
LQW-L	1	R GMd	0.06 (0.02–0.13)	0.02 (0.00–0.05)	-0.48	0.016	KOA↑
SZS	3	R VM	0.00 (0.00–0.03)	0.09 (0.02–0.25)	0.56	0.004	HC↑
YMFZ-R	3	L MG	0.18 (0.07–0.54)	0.03 (0.02–0.09)	-0.50	0.037	KOA↑
YMFZ-R	5	L RF	0.10 (0.05–0.17)	0.04 (0.00–0.07)	-0.47	0.038	KOA↑
YMFZ-R	5	L VL	0.16 (0.09–0.29)	0.03 (0.01–0.09)	-0.44	0.038	KOA↑
YMFZ-R	5	R GMd	0.05 (0.01–0.15)	0.01 (0.00–0.02)	-0.43	0.038	KOA↑
YS-L	1	L TA	0.02 (0.00–0.11)	0.13 (0.07–0.17)	0.56	0.010	HC↑
YS-R	1	R GMx	0.09 (0.05–0.15)	0.04 (0.02–0.07)	-0.51	0.041	KOA↑

Abbreviations: KOA, knee osteoarthritis; HC, healthy controls; FDR, false discovery rate; IQR, interquartile range; Cond., analysis condition; Syn, synergy; L/R, left/right. Muscle and movement abbreviations are defined in the List of abbreviations. Up arrows mark the group with the higher median loading. Complete statistics are in `Supplementary_Tables.xlsx` (sheet `S5_muscle_weights`).

3.5 Activation profiles differ in a subset of synergies

Group differences in activation profiles were detected in 26/99 synergies, comprising 34 cluster-corrected significant windows; 24 (71%) reflected higher activation in KOA and 10 higher activation in HC (Fig. 5; affected condition–synergy pairs and per-window results are listed in Additional file 1: Tables S6 and S7).

Window count and total duration identified different movements (Additional file 1: Fig. S21). By window count, Repulse Monkey was most affected (10 windows, all KOA-higher; Fig. 5a), whereas by total significant duration Cloud Hands dominated (125% of the cycle across six longer, bidirectional windows; Fig. 5b). The two directions also differed in temporal extent: KOA-higher windows were brief (median 7.8% of the cycle, IQR 6.1–10.5), whereas HC-higher windows were roughly twice as long (median 16.8%, IQR 11.0–24.9; Mann–Whitney $p = 0.007$). The duration-normalised absolute cluster statistic (absolute cluster mass divided by the number of time points) was slightly higher for KOA-higher than HC-higher windows (median 3.3 versus 3.1; exploratory Mann–Whitney $p = 0.030$), whereas HC-higher windows had larger absolute mass

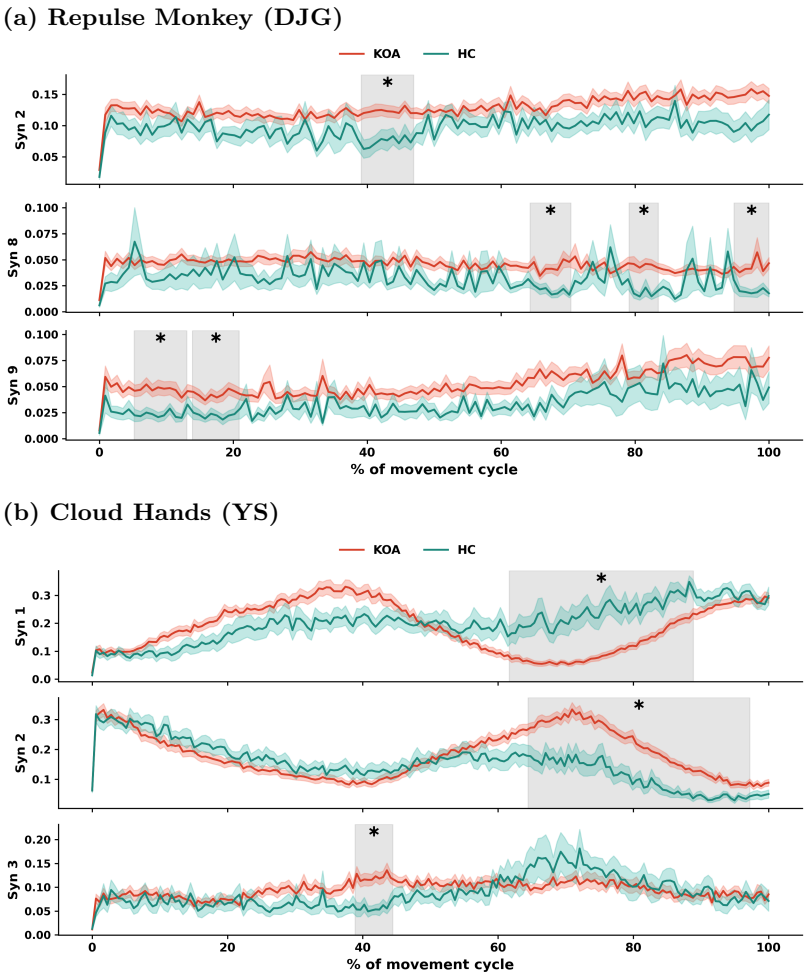


Fig. 5 Synergy activation profiles over the movement cycle, KOA versus HC (mean ± standard error; coral = KOA, teal = HC); shaded regions and asterisks indicate cluster-level permutation-significant windows (cluster-corrected $p < 0.05$; no additional across-synergy FDR correction). Only synergies with at least one significant window are shown (full set for all conditions in Additional file 1: Fig. S20). The two movements illustrate the complementary metrics: **(a)** DJG has the most windows but they are short and all KOA-higher, whereas **(b)** YS has the longest cumulative duration, with bidirectional activation-profile differences (both KOA- and HC-higher windows). Abbreviations: KOA, knee osteoarthritis; HC, healthy controls; FDR, false discovery rate; DJG, Repulse Monkey; YS, Cloud Hands.

because they were longer. These statistics describe standardised group separation, not activation intensity. Cumulatively, KOA-higher windows had a greater summed duration than HC-higher windows (229 versus 175 cycle-percent units), and differences concentrated in the mid-to-late movement cycle (25/34 windows with midpoint beyond 33%).

Table 4 Activation-profile summary by movement. Significant synergies are condition–synergy pairs with at least one cluster-corrected window. The KOA and HC window columns give the number of significant windows with higher activation in each group; the corresponding duration columns give their cumulative durations in cycle-percent units, summed across movement-side conditions and synergies. These are durations of between-group differences, not group-specific activation durations, and can exceed 100% because overlapping windows in different synergies are counted separately. A window may reflect amplitude, profile shape or phase. Minimum p_{corr} is the smallest cluster-corrected p value among the movement's significant windows. Full per-window start/end times, directions and cluster-corrected p values are i n Additional file 1: Table S7.

Mov.	Sig. syn.	Windows, n		Cumulative duration (% cycle)		Minimum p_{corr}
		KOA↑	HC↑	KOA↑	HC↑	
DJ	2	0	2	0.0	53.6	0.007
DJG	6	10	0	67.8	0.0	0.007
JJDL	2	0	2	0.0	24.7	0.017
LQW	4	4	2	34.4	14.9	0.003
LXAB	3	4	0	42.1	0.0	0.003
YMFZ	4	3	1	29.3	12.0	0.007
YS	5	3	3	55.6	69.4	< 0.001

Abbreviations: KOA, knee osteoarthritis; HC, healthy controls; Mov., movement; Sig. syn., significant synergies; p_{corr}, cluster-corrected p value; ↑, higher activation. Movement codes are defined in the List of abbreviations.

Among the affected synergies, KOA-higher activation-profile windows often occurred in those weighted toward the gluteals, hamstrings and gastrocnemius, whereas quadriceps-weighted synergies showed windows in both directions (Additional file 1: Table S9). A complementary per-subject analysis of synergy peak-activation timing (permutation test on the circular mean direction, FDR-corrected across 99 synergies) showed no systematic shift in peak location (0/99 synergies after FDR; smallest BH-FDR-adjusted $p = 0.099$; Additional file 1, Section S7).

3.6 Functional contribution and key-muscle profile

Across all movements, the quadriceps made the largest contribution to the reconstructed EMG envelope (Fig. 6; exact values in Additional file 1: Table S11). The ten muscles with the largest contributions made up 71.9% of the summed reconstructed EMG envelope; the left and right vastus lateralis, vastus medialis and rectus femoris together accounted for ≈49% of the summed reconstructed EMG envelope. When each participant's contribution was averaged across movements, none of the 16 muscle-level KOA–HC comparisons was significant after BH-FDR correction (lowest adjusted p value = 0.574; Fig. 6).

When each movement was examined separately, functional contribution differed between groups in 11/272 muscle×condition comparisons after global BH-FDR correction (Fig. 7, Table 5). KOA had a higher relative gluteus medius contribution in two

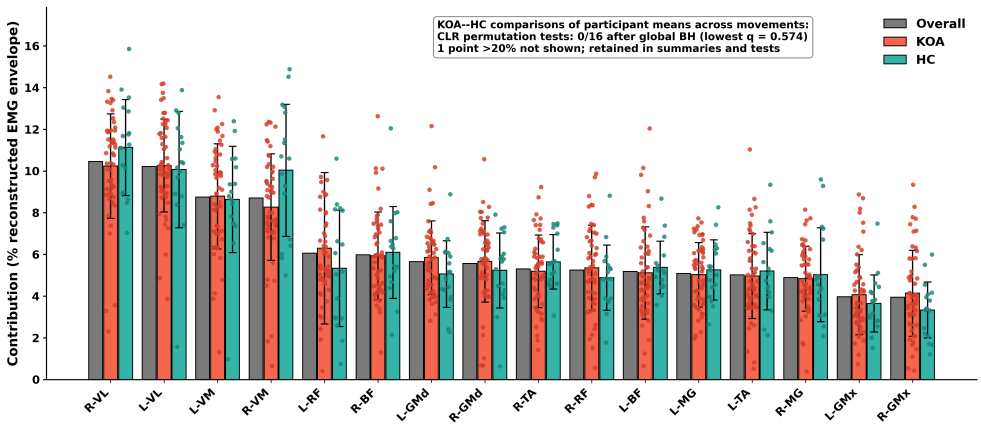


Fig. 6 Key-muscle contribution profile: each muscle's estimated percentage of the summed reconstructed EMG envelope across all movements, ranked in descending order. Grey bars show the mean across all participants; coloured bars show group means, error bars SD and dots individual participant means across movements. One L-RF value (26.9%) is not shown as a dot so that the other values remain easy to see, but it is still included in the means, SDs and statistical tests. KOA–HC inference used a studentized label-permutation test on centered-log-ratio (CLR)-transformed 16-part compositions, with BH-FDR correction across the 16 muscles; none was significant (0/16, lowest adjusted p value = 0.574). Abbreviations: KOA, knee osteoarthritis; HC, healthy controls; CLR, centered log ratio; SD, standard deviation; FDR, false discovery rate; BF, biceps femoris; MG, medial gastrocnemius; GMx, gluteus maximus; GMd, gluteus medius; RF, rectus femoris; TA, tibialis anterior; VL, vastus lateralis; VM, vastus medialis; L/R prefixes denote left/right side.

conditions; HC had higher relative contributions from tibialis anterior, vastus medialis, biceps femoris, medial gastrocnemius or rectus femoris in selected conditions. The 11 primary differences occurred in four movements: Heel Kick, Golden Rooster Stands on One Leg, Grasp the Sparrow's Tail, and Cross Hands. An exploratory within-condition correction identified 14 comparisons in total, adding three findings that did not survive the global correction (`Supplementary_Tables.xlsx`, sheet `S10-S11_functional_contribution`).

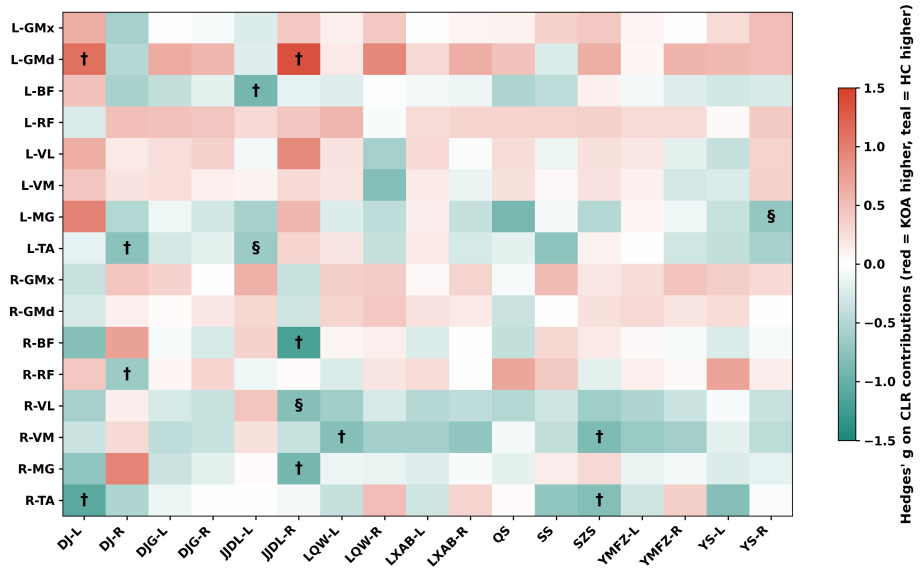


Fig. 7 Functional-contribution differences between KOA and HC for each muscle and condition. Each square shows the effect-size direction and magnitude for one muscle×condition comparison: red indicates a higher relative contribution in KOA, teal indicates a higher relative contribution in HC, and darker colour indicates a larger between-group difference. Effect sizes are Hedges' g calculated on CLR-transformed contributions (positive = KOA higher); the colour scale spans −1.5 to 1.5. Muscles are ordered from proximal to distal, with the left-side channels followed by the right-side channels in the same order. A dagger (†) marks a muscle×condition comparison that remained significant (BH-adjusted $p < 0.05$) after all 272 comparisons were adjusted together in the primary analysis. A section sign (§) marks one of three additional comparisons that was significant only after the 16 muscles within the same condition were adjusted together in the exploratory analysis. Abbreviations and marks: KOA, knee osteoarthritis; HC, healthy controls; CLR, centered log ratio; FDR, false discovery rate; BF, biceps femoris; MG, medial gastrocnemius; GMx, gluteus maximus; GMd, gluteus medius; RF, rectus femoris; TA, tibialis anterior; VL, vastus lateralis; VM, vastus medialis; L/R prefixes denote left/right side; QS, Opening Form; DJG, Repulse Monkey; LXAB, Brush Knee and Twist Step; YMFZ, Part the Wild Horse's Mane; YS, Cloud Hands; JJDL, Golden Rooster Stands on One Leg; DJ, Heel Kick; LQW, Grasp the Sparrow's Tail; SZS, Cross Hands; SS, Closing Form; L/R, left/right stance leg; NA, single-stance movement.

Table 5 Muscle×condition functional-contribution comparisons that were significant after the primary global BH-FDR correction across all 272 comparisons. Each row is one analysis condition (movement–stance side; SZS is single-stance). Raw percentage contributions are reported descriptively as mean (SD), whereas inference used a 9,999-resample studentized label-permutation test on CLR-transformed compositions. Available-case sample sizes per condition ranged from 41 to 52 KOA and 12 to 17 HC participants without imputation. Hedges' g and its pointwise 95% bootstrap CI are also on the CLR scale and are oriented KOA minus HC; the final column reports BH-adjusted p values for the primary global family of 272 comparisons, whereas the CIs are not multiplicity-adjusted. The complete 272-row analysis, including the exploratory within-condition sensitivity correction, is in `Supplementary_Tables.xlsx`, sheet `S10-S11_functional_contribution`.

Cond.	Muscle	KOA (%)	HC (%)	g [95% CI]	BH-adjusted p
DJ-L	L-GMd	7.36 (1.97)	4.93 (1.97)	1.10 [0.51, 1.83]	0.047
DJ-L	R-TA	5.98 (1.71)	7.60 (1.80)	−1.07 [−1.70, −0.65]	0.032
DJ-R	L-TA	6.02 (2.50)	7.58 (2.13)	−0.77 [−1.18, −0.43]	0.032
DJ-R	R-RF	7.60 (2.65)	9.87 (2.66)	−0.66 [−1.42, −0.36]	0.039
JJDL-L	L-BF	8.03 (4.00)	11.08 (2.55)	−0.90 [−1.31, −0.56]	0.032
JJDL-R	L-GMd	6.54 (2.24)	3.65 (1.75)	1.35 [0.81, 2.03]	0.032
JJDL-R	R-BF	8.83 (3.47)	13.29 (5.30)	−1.18 [−1.87, −0.60]	0.032
JJDL-R	R-MG	7.00 (2.78)	9.49 (4.46)	−0.90 [−1.47, −0.47]	0.034
LQW-L	R-VM	11.07 (3.66)	14.72 (3.32)	−0.80 [−1.30, −0.47]	0.027
SZS	R-TA	5.54 (2.94)	7.49 (1.90)	−0.82 [−1.23, −0.42]	0.034
SZS	R-VM	7.57 (2.79)	11.05 (4.13)	−0.85 [−1.36, −0.41]	0.046

Abbreviations: KOA, knee osteoarthritis; HC, healthy controls; CI, confidence interval; CLR, centered log ratio; FDR, false discovery rate; g, Hedges' g; BF, biceps femoris; MG, medial gastrocnemius; GMx, gluteus maximus; GMd, gluteus medius; RF, rectus femoris; TA, tibialis anterior; VL, vastus lateralis; VM, vastus medialis; L/R prefixes denote left/right side; QS, Opening Form; DJG, Repulse Monkey; LXAB, Brush Knee and Twist Step; YMFZ, Part the Wild Horse's Mane; YS, Cloud Hands; JJDL, Golden Rooster Stands on One Leg; DJ, Heel Kick; LQW, Grasp the Sparrow's Tail; SZS, Cross Hands; SS, Closing Form; L/R, left/right stance leg; NA, single-stance movement. Positive g indicates KOA higher; negative g indicates HC higher.

3.7 Composite movement ranking

Because its five components were standardised across the 17 conditions and equally weighted, S_c is a relative descriptive index, not a test statistic or diagnostic score. Across the 17 movement–stance-side conditions, the left-stance condition of Heel Kick (DJ-L) had the highest composite synergy index (S_c = 0.96), followed by the right-stance conditions of Repulse Monkey (DJG-R; S_c = 0.78), Heel Kick (DJ-R; S_c = 0.61), and Golden Rooster Stands on One Leg (JJDL-R; S_c = 0.45; Fig. 8). DJ-L was distinguished primarily by functional contribution, with additional above-average differences in synergy number and muscle weights. By contrast, DJG-R was distinguished by structural divergence and synergy number despite a below-average contribution difference. Cloud Hands had the largest activation-profile scores (YS-L and YS-R) but ranked fifth and sixth overall because its other components were mostly near or below the across-condition average. Similarly, JJDL-L had the largest muscle-weight score but a composite index near zero. Thus, no single measure reproduced the integrated ranking.

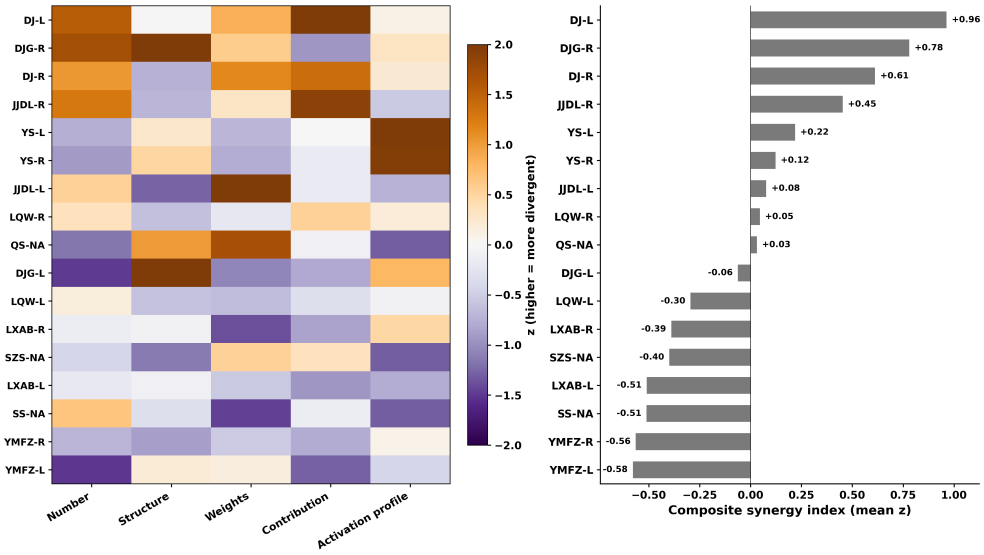


Fig. 8 Composite ranking of the 17 movement–stance-side conditions across five synergy measures. Conditions are ordered by the composite synergy index. **Left:** Per-measure KOA–HC divergence, standardised as z-scores across conditions (orange = greater-than-average divergence; purple = less-than-average divergence). **Right:** Composite synergy index (grey bars, equal-weighted mean of the five z-scores; values annotated). Higher values indicate greater overall KOA–HC divergence relative to the other conditions. The composite ranking is descriptive and has no built-in significance threshold. Condition labels use movement–stance-side notation; NA denotes conditions without a separate left/right stance-side designation. Abbreviations: KOA, knee osteoarthritis; HC, healthy controls; QS, Opening Form; DJG, Repulse Monkey; LXAB, Brush Knee and Twist Step; YMFZ, Part the Wild Horse's Mane; YS, Cloud Hands; JJDL, Golden Rooster Stands on One Leg; DJ, Heel Kick; LQW, Grasp the Sparrow's Tail; SZS, Cross Hands; SS, Closing Form; L/R, left/right stance leg; NA, single-stance movement. Full per-measure z-scores and composite values are in Additional file 1: Table S12.

4 Discussion

Across the five measures, detected KOA–HC differences were concentrated in synergy recruitment rather than spatial architecture (Table 6). The groups had broadly similar muscle groupings but differed selectively in relative muscle contribution and activation profiles. Because the study was cross-sectional, these are observed group associations, not evidence that KOA caused the differences.

Table 6 Summary of the five analysis measures. Synergy number, similarity and muscle weights describe synergy structure; functional contribution and activation profiles describe how the synergies are used. Structure was similar between groups, whereas recruitment differed in selected comparisons. Per-movement activation-profile counts are given in Table 4.

Category	Measure	Result	Summary
Structure	Synergy number	0/17 conditions significant (FDR)	No detected difference
Structure	Synergy similarity	95/125 pairs: cosine ≥ 0.80	Mostly similar
Structure	Muscle weights	25/1584 weights differed (1.6%)	Sparse differences
Use	Functional contribution	11/272 significant (global FDR)	Selective differences
Use	Activation profiles	26/99 synergies; 34 windows (24 KOA↑)	Selective differences

Abbreviations: KOA, knee osteoarthritis; HC, healthy controls; FDR, false discovery rate. The functional-contribution count uses the primary global BH-FDR family across all 272 muscle×condition comparisons.

4.1 Key muscles and broadly similar modular control

Across the routine, the quadriceps contributed approximately 49% of the summed reconstructed EMG envelope, and the global basis contained six left–right paired modules, with secondary contributions from the gluteal/posterior-chain muscles and tibialis anterior (Figs. 2 and 6; exact values in Additional file 1: Table S11). This modular pattern is consistent with Tai Chi gait mechanics relative to normal walking: longer single-leg stance, greater knee flexion and larger lateral body shift [32]; larger mediolateral shear forces and frontal-plane knee and hip moments [33]; and greater knee-extensor, hip-abductor and ankle-dorsiflexor activation [32, 34]. The module labels are functional interpretations of EMG covariation, however, and do not directly measure muscle force or joint function.

The paired modules may provide a common pattern for alternating supporting and moving limbs: knee-extension modules can contribute to support of a flexed knee, hip/posterior-chain modules to postural control, and tibialis-anterior modules to foot clearance and placement. More generally, modular-control evidence has been reported in frog defensive kicking, human walking and primate reaching and grasping [11]. In bullfrogs, most swimming and jumping muscle synergies were preserved after deafferentation, some were shared between the two behaviours, and deafferentation altered the amplitude and temporal patterns of the activation coefficients of most shared synergies [19]. These findings support centrally organised spatial modules whose recruitment is modulated by task and sensory feedback.

Between groups, no condition showed a difference in synergy number after FDR correction; most matched synergies met the prespecified similarity threshold; and only a small proportion of muscle weights differed (25/1584; 1.6%; Figs. 3 and 4; Table 3). These findings are consistent with broadly similar spatial architecture but do not demonstrate equivalence or complete preservation. This overall pattern contrasts descriptively with the fewer, merged motor modules reported during post-stroke walking [16] and with the fractionation of running synergies during child-to-adult development and their merging with adult running experience and training [17]. However, those studies used different participants, tasks and methods, so this comparison is only descriptive and does not by itself prove that module architecture is preserved in KOA.

Stance side still mattered within movements. Synergy number differed between left- and right-stance conditions in four of seven bilateral movements, and these side effects were mostly shared by KOA and HC. This suggests that synergy number depended more on the role assigned to the stance limb than on disease status. Tai Chi gait involves prolonged single-leg support and large lateral body shifts [32], while different Tai Chi movements impose distinct joint and muscle demands [34]. Given these biomechanical demands, changing the stance side may alter balance and movement requirements even within the same named movement.

Repulse Monkey was the only movement with a significant side×group interaction, indicating that its left–right contrast differed between groups. Follow-up paired comparisons showed a higher synergy number during right than left stance in HC, but no side difference in KOA. This pattern is consistent with reduced task-related lateralisation in KOA; however, without information on limb dominance, symptom side or movement kinematics, its mechanism cannot be determined.

Heel Kick and Golden Rooster Stands on One Leg showed significant group main effects averaged across stance sides, with higher synergy numbers in KOA and no side×group interactions. However, none of the separate KOA–HC comparisons within a stance side survived FDR correction. These results therefore support group differences averaged across sides, but do not identify an effect specific to either limb. Modelling stance side explicitly was important because treating the two conditions as interchangeable would have hidden the side-dependent patterns.

4.2 Selective KOA–HC differences in synergy recruitment and activation profiles

Among the globally significant functional-contribution comparisons, gluteus medius was KOA-higher in two conditions, whereas the other nine comparisons were HC-higher (Fig. 7; Table 5). Thus, differences were detected only for specific muscles and conditions. Because the 16 contributions sum to 100% and are computed over the full movement cycle, they reflect each muscle's relative share of the total rather than its absolute activation, force, or joint loading. They also do not indicate when during the cycle a difference occurred.

Given the single-leg and weight-transfer demands of Tai Chi, the KOA-higher gluteus medius contribution in Heel Kick and Golden Rooster Stands on One Leg is compatible with greater *relative* reliance on the hip abductor to maintain balance

during stance. A cross-sectional study found lower maximal isometric strength across the hip muscle groups, including the abductors, in people with symptomatic medial KOA than in asymptomatic controls [9]. This weakness provides a plausible context for altered hip-muscle use during stance, although the cited study did not examine muscle recruitment. The present data cannot distinguish compensation from an alternative task strategy or a compositional shift. Conversely, the HC-higher differences involved ankle, knee-extensor and posterior-chain muscles, not a uniform increase or decrease across the limb. This mixed, task-specific pattern is consistent with walking studies showing that KOA-related co-activation and EMG waveform differences depend on the muscle examined and the clinical severity group [10, 35].

Activation-profile differences were likewise localised to specific portions of the movement cycle, without a systematic between-group shift in peak timing. One possible modular-control explanation comes from standing-balance perturbation research, in which the temporal recruitment of spatially fixed synergies was well reconstructed using delayed feedback derived from centre-of-mass kinematics [15]. In Tai Chi, phase-specific muscle-synergy patterns have also been identified during the knee-lift, extension and recovery phases of a leg-stirrup movement [6]. Accordingly, the cycle-localised differences observed here are compatible with group differences in the temporal modulation of largely shared modules as limb roles, support demands and posture change during a movement. The observed distribution—more, typically shorter KOA-higher windows and fewer, longer HC-higher windows—indicates that group differences were localised within the time-normalised movement cycle and did not follow a uniform directional pattern across significant windows.

4.3 Dynamic weight-transfer movements show KOA-associated neuromuscular differences

No movement was the most KOA-divergent on every measure. Heel Kick was distinguished mainly by relative contribution, Golden Rooster Stands on One Leg by several recruitment differences, Repulse Monkey by lower synergy similarity and brief activation-profile windows, and Cloud Hands by fewer but longer activation-profile windows. These signatures are not contradictory: contribution is cycle-integrated, activation profiles are cycle-localised, and the structural measures address the composition of the modules themselves.

The highest-ranked movements share demanding, asymmetric weight-transfer requirements: single-leg support in Heel Kick and Golden Rooster Stands on One Leg, backward stepping in Repulse Monkey, and continuous lateral shifting in Cloud Hands. These characteristics align with prior biomechanical evidence of prolonged single-leg support and large lateral body displacement during Tai Chi gait [32], movement-specific joint and muscle demands across Tai Chi forms [34], and phase-specific synergy patterns during a leg-stirrup movement [6]. The integrated index therefore provides a practical basis for prioritising candidate tasks in future KOA research, while remaining a relative descriptive summary without a significance threshold or validated diagnostic interpretation.

4.4 Clinical implications

These findings identify priorities for rehabilitation research. Knee extensors accounted for approximately 49% of the reconstructed EMG across the Tai Chi routine, whereas task-specific group differences also involved the gluteus medius, tibialis anterior, vastus medialis, biceps femoris, medial gastrocnemius and rectus femoris. Future trials could therefore test whole-limb strengthening programmes that combine knee-extensor work with exercises for the hip abductors, hamstrings, calf muscles and ankle dorsiflexors; direct strength and functional assessments should guide individual prescription. In people with medial KOA and varus malalignment, a 12-week hip abductor and adductor strengthening programme improved pain, physical function and muscle strength but did not change the peak external knee adduction moment [36]. A separate trial found similar improvements in pain and physical function after neuromuscular and quadriceps-strengthening programmes, with neither programme changing the knee adduction moment [37]. Because relative EMG contribution does not measure muscle strength, the contribution results identify muscles for targeted assessment rather than demonstrating weakness.

The predominance of KOA–HC differences in synergy recruitment rather than synergy structure supports evaluating task-specific motor-control training. Such training could target smooth weight transfer, single-leg balance, foot placement and coordinated control of the hip, knee and ankle. In a secondary analysis of a randomised trial, 12 weeks of neuromuscular training produced greater reductions in medial and lateral quadriceps–hamstring co-contraction during walking than quadriceps-strengthening exercise [38]. A separate randomised trial found that Tai Chi and standard physical therapy produced comparable improvements in knee pain and physical function [39].

For KOA assessment research, Heel Kick and Repulse Monkey emerge as the leading candidate tasks from the composite ranking, while Golden Rooster Stands on One Leg and Cloud Hands offer complementary challenges. Single-leg standing balance in medial KOA is associated with knee pain, lower-limb alignment and quadriceps strength [40]. During a single-limb mini-squat, people with KOA showed higher medial gastrocnemius and tibialis anterior activity during descent and higher medial gastrocnemius and gluteus medius activity during ascent than healthy controls [41]. Before incorporating these Tai Chi tasks into clinical assessment, their safety, test–retest reliability, associations with symptoms and joint mechanics, responsiveness to change and clinically useful cut-points should be established in an independent sample.

4.5 Limitations

Several limitations should be considered. First, the cross-sectional design permits between-group comparisons but cannot establish causality or temporal change. Second, the HC group was smaller than the KOA group, and participant numbers varied slightly across conditions. Analyses were conducted at the subject level using statistical tests suited to unequal group sizes and false-discovery-rate control; nevertheless, estimates for the HC group remain less precise. Third, surface EMG and NMF provide indirect, model-dependent characterisations of muscle coordination. Surface EMG is influenced by spatial sampling and signal-processing choices [42], whereas the extracted

synergies and their number depend on the factorisation method and model-order criterion [13]. These modules are descriptive decompositions of EMG rather than direct measurements of neural commands, and their neural implementation remains debated [43]. Fourth, joint mechanics and detailed clinical-severity measures were not incorporated into the present analysis, so the proposed biomechanical interpretations remain to be tested. Finally, the findings are limited to the participants and Tai Chi routine studied, and the exploratory combined movement ranking requires validation in an independent sample.

Future studies should replicate these muscle- and movement-specific findings in larger, more balanced samples using standardised definitions of stance side and movement phase. Synchronised motion capture, force measurements, muscle-strength testing and validated measures of pain and function would clarify the biomechanical and clinical significance of the recruitment differences. Longitudinal and interventional designs could then determine whether the candidate features change with Tai Chi training and track clinical outcomes or radiographic progression.

5 Conclusions

Across the eight-form routine, Tai Chi engaged a compact set of key lower-limb muscles dominated by the quadriceps (≈49% of the reconstructed EMG envelope) and organised into six bilaterally symmetric synergy modules. The modular architecture was broadly similar in KOA and controls: synergy number, overall similarity and muscle weights differed minimally between groups, consistent with broadly conserved spatial composition. The observed differences were selective and movement-specific, concentrated in recruitment rather than structure: within these largely shared synergies, relative muscle contribution and activation profiles changed in particular muscles and cycle windows rather than uniformly across the limb, most evidently during dynamic weight-transfer movements. No single measure captured the full pattern across movements; a descriptive integrated index of all five measures identified Heel Kick and Repulse Monkey as showing the greatest overall KOA–HC divergence, with Golden Rooster Stands on One Leg and Cloud Hands also prominent. These findings nominate specific muscles—particularly the knee extensors, together with the hip abductors, hamstrings, calf muscles and ankle dorsiflexors— and specific movements as candidates for task-specific motor-control training and for compact KOA assessment batteries.

List of abbreviations

ACR: American College of Rheumatology; ANOVA: Analysis of variance; BF: Biceps femoris; BMI: Body-mass index; FDR: False discovery rate; GMd: Gluteus medius; GMx: Gluteus maximus; HC: Healthy control; IQR: Interquartile range; KL: Kellgren–Lawrence radiographic grade; KOA: Knee osteoarthritis; L/R: Left/right stance leg; MG: Medial gastrocnemius; NA: Not applicable (single-stance movement); NMF: Non-negative matrix factorization; NNDSVD: Non-negative double singular value decomposition; OARSI: Osteoarthritis Research Society International; RF: Rectus femoris; RFT: Random-field theory; SD: Standard deviation; sEMG: Surface electromyography; SPM: Statistical parametric mapping; TA: Tibialis anterior; VAF:

Variance accounted for; VL: Vastus lateralis; VM: Vastus medialis; WOMAC: Western Ontario and McMaster Universities Osteoarthritis Index. Movement abbreviations: QS: Opening Form; DJG: Repulse Monkey; LXAB: Brush Knee and Twist Step; YMFZ: Part the Wild Horse's Mane; YS: Cloud Hands; JJDL: Golden Rooster Stands on One Leg; DJ: Heel Kick; LQW: Grasp the Sparrow's Tail; SZS: Cross Hands; SS: Closing Form.

Ethics approval and consent to participate. The study protocol, informed-consent form and participant-recruitment materials were approved by the Ethics Review Committee of the Rehabilitation Hospital Affiliated to Fujian University of Traditional Chinese Medicine (approval no. 2024KY-038-01). All methods were performed in accordance with the principles of the Declaration of Helsinki and with applicable institutional guidelines and regulations. All participants provided written informed consent before participation.

Consent for publication. Not applicable.

Data availability. The de-identified participant-level baseline data, detailed condition-level results, supplementary figures and methodological information supporting the findings of this study are included in Additional file 1 (`Additional_file_1.pdf`). The complete machine-readable statistical results are included in `Supplementary_Tables.xlsx`. The raw surface-electromyography datasets generated and/or analysed during the current study are not publicly available to protect participant privacy but are available from the corresponding authors on reasonable request.

Competing interests. The authors declare that they have no competing interests.

Funding. This work was supported by the National Natural Science Foundation of China (grant nos. 12572368, 82405535 and 82575192); the Natural Science Foundation of Fujian Province (grant no. 2026J001913); the Fuzhou Science and Technology Project (grant nos. 2025-P-005 and 2025E3005); the 2025 Ningbo University High-Level Science and Technology Project Incubation Program (grant no. GJPY2025027); the Foundation of the Key Laboratory of Orthopedics and Traumatology of Traditional Chinese Medicine and Rehabilitation, Ministry of Education, Fujian University of Traditional Chinese Medicine (grant no. XGS2024004); and the K. C. Wong Magna Fund at Ningbo University.

Authors' contributions. Ye Ma and Meijin Hou designed the study; Shengxing Fu, Xiangbin Wang and Meijin Hou collected the data; Meijin Hou, Dongwei Liu and Ye Ma analysed the data and drafted the manuscript; Xiangbin Wang, Meijin Hou, Dongwei Liu and Ye Ma interpreted the results; Dongwei Liu, Chenyi Guo, Meijin Hou, Shengxing Fu, Xiangbin Wang and Ye Ma revised the manuscript; all authors revised and approved the final manuscript.

Acknowledgements. The authors sincerely thank all participants—both individuals with knee osteoarthritis and healthy volunteers—for their time, effort and willingness to perform the Tai Chi routine while surface electromyography was recorded. This study would not have been possible without their contribution.

References

[1] Roos EM, Arden NK. Strategies for the prevention of knee osteoarthritis. Nature Reviews Rheumatology. 2016;12(2):92–101. https://doi.org/10.1038/nrrheum.2015.135.

[2] Katz JN, Arant KR, Loeser RF. Diagnosis and treatment of hip and knee osteoarthritis: a review. JAMA. 2021;325(6):568–578. https://doi.org/10.1001/jama.2020.22171.

[3] Song R, Lee EO, Lam P, Bae SC. Effects of tai chi exercise on pain, balance, muscle strength, and perceived difficulties in physical functioning in older women with osteoarthritis: a randomized clinical trial. The Journal of Rheumatology. 2003;30(9):2039–2044. Available at https://www.jrheum.org/content/30/9/2039.

[4] Kolasinski SL, Neogi T, Hochberg MC, Oatis C, Guyatt G, Block J, et al. 2019 American College of Rheumatology/Arthritis Foundation Guideline for the Management of Osteoarthritis of the Hand, Hip, and Knee. Arthritis Care & Research. 2020;72(2):149–162. https://doi.org/10.1002/acr.24131.

[5] Bannuru RR, Osani MC, Vaysbrot EE, Arden NK, Bennell K, Bierma-Zeinstra SMA, et al. OARSI guidelines for the non-surgical management of knee, hip, and polyarticular osteoarthritis. Osteoarthritis and Cartilage. 2019;27(11):1578–1589. https://doi.org/10.1016/j.joca.2019.06.011.

[6] Zhang X, Jia M, Ke Y, Zhou J. Neuromuscular synergy characteristics of Tai Chi leg stirrup movements: optimal coordination patterns throughout various phases. Frontiers in Bioengineering and Biotechnology. 2024;12:1482793. https://doi.org/10.3389/fbioe.2024.1482793.

[7] Wayne PM, Gow BJ, Hou F, Ma Y, Hausdorff JM, Lo J, et al. Tai Chi training's effect on lower extremity muscle co-contraction during single- and dual-task gait: Cross-sectional and randomized trial studies. PLOS ONE. 2021;16(1):e0242963. https://doi.org/10.1371/journal.pone.0242963.

[8] Alnahdi AH, Zeni JA, Snyder-Mackler L. Muscle impairments in patients with knee osteoarthritis. Sports Health. 2012;4(4):284–292. https://doi.org/10.1177/1941738112445726.

[9] Hinman RS, Hunt MA, Creaby MW, Wrigley TV, McManus FJ, Bennell KL. Hip muscle weakness in individuals with medial knee osteoarthritis. Arthritis Care & Research. 2010;62(8):1190–1193. https://doi.org/10.1002/acr.20199.

[10] Hubley-Kozey CL, Hill NA, Rutherford DJ, Dunbar MJ, Stanish WD. Co-activation differences in lower limb muscles between asymptomatic controls and those with varying degrees of knee osteoarthritis during walking. Clinical Biomechanics. 2009;24(5):407–414. https://doi.org/10.1016/j.clinbiomech.2009.

02.005.

[11] Bruton M, O'Dwyer N. Synergies in coordination: a comprehensive overview of neural, computational, and behavioral approaches. Journal of Neurophysiology. 2018;120(6):2761–2774. https://doi.org/10.1152/jn.00052.2018.

[12] Lee DD, Seung HS. Learning the parts of objects by non-negative matrix factorization. Nature. 1999;401(6755):788–791. https://doi.org/10.1038/44565.

[13] Tresch MC, Cheung VCK, d'Avella A. Matrix factorization algorithms for the identification of muscle synergies: evaluation on simulated and experimental data sets. Journal of Neurophysiology. 2006;95(4):2199–2212. https://doi.org/10.1152/jn.00222.2005.

[14] Spüler M, Irastorza-Landa N, Sarasola-Sanz A, Ramos-Murguialday A. Extracting Muscle Synergy Patterns from EMG Data Using Autoencoders. In: Artificial Neural Networks and Machine Learning – ICANN 2016. vol. 9887 of Lecture Notes in Computer Science. Cham: Springer; 2016. p. 47–54.

[15] Safavynia SA, Ting LH. Task-level feedback can explain temporal recruitment of spatially fixed muscle synergies throughout postural perturbations. Journal of Neurophysiology. 2012;107(1):159–177. https://doi.org/10.1152/jn.00653.2011.

[16] Clark DJ, Ting LH, Zajac FE, Neptune RR, Kautz SA. Merging of healthy motor modules predicts reduced locomotor performance and muscle coordination complexity post-stroke. Journal of Neurophysiology. 2010;103(2):844–857. https://doi.org/10.1152/jn.00825.2009.

[17] Cheung VCK, Cheung BMF, Zhang JH, Chan ZYS, Ha SCW, Chen CY, et al. Plasticity of muscle synergies through fractionation and merging during development and training of human runners. Nature Communications. 2020;11(1):4356. https://doi.org/10.1038/s41467-020-18210-4.

[18] Frère J, Hug F. Between-subject variability of muscle synergies during a complex motor skill. Frontiers in Computational Neuroscience. 2012;6:99. https://doi.org/10.3389/fncom.2012.00099.

[19] Cheung VCK, d'Avella A, Tresch MC, Bizzi E. Central and sensory contributions to the activation and organization of muscle synergies during natural motor behaviors. Journal of Neuroscience. 2005;25(27):6419–6434. https://doi.org/10.1523/JNEUROSCI.4904-04.2005.

[20] Shourijeh MS, Flaxman TE, Benoit DL. An approach for improving repeatability and reliability of non-negative matrix factorization for muscle synergy analysis. Journal of Electromyography and Kinesiology. 2016;26:36–43. https://doi.org/10.1016/j.jelekin.2015.12.001.

[21] Brunet JP, Tamayo P, Golub TR, Mesirov JP. Metagenes and molecular pattern discovery using matrix factorization. Proceedings of the National Academy of Sciences. 2004;101(12):4164–4169. https://doi.org/10.1073/pnas.0308531101.

[22] Zhang Z, Huang C, Jiang Q, Zheng Y, Liu Y, Liu S, et al. Guidelines for the diagnosis and treatment of osteoarthritis in China (2019 edition). Annals of Translational Medicine. 2020;8(19):1213. https://doi.org/10.21037/atm-20-4665.

[23] Yue H, Li Y, Ma J, Xie C, Xie F, Cai J, et al. Effect of Tai Chi on knee pain and muscle strength in middle-aged and older adults with knee osteoarthritis: a randomized controlled trial protocol. BMC Complementary Medicine and Therapies. 2023;23(1):256. https://doi.org/10.1186/s12906-023-04070-0.

[24] SENIAM. SENIAM: Surface ElectroMyoGraphy for the Non-Invasive Assessment of Muscles — recommendations for sensor locations on individual muscles [Web page]; n.d. [cited 24 June 2026]. Available from: http://www.seniam.org/.

[25] Boutsidis C, Gallopoulos E. SVD based initialization: A head start for nonnegative matrix factorization. Pattern Recognition. 2008;41(4):1350–1362. https://doi.org/10.1016/j.patcog.2007.09.010.

[26] Aitchison J. The Statistical Analysis of Compositional Data. London: Chapman and Hall; 1986.

[27] Janssen A. Studentized permutation tests for non-i.i.d. hypotheses and the generalized Behrens–Fisher problem. Statistics & Probability Letters. 1997;36(1):9–21. https://doi.org/10.1016/S0167-7152(97)00043-6.

[28] Kerby DS. The simple difference formula: An approach to teaching nonparametric correlation. Comprehensive Psychology. 2014;3:11.IT.3.1. https://doi.org/10.2466/11.IT.3.1.

[29] Hedges LV. Distribution theory for Glass's estimator of effect size and related estimators. Journal of Educational Statistics. 1981;6(2):107–128. https://doi.org/10.3102/10769986006002107.

[30] Efron B, Tibshirani RJ. An Introduction to the Bootstrap. vol. 57 of Monographs on Statistics and Applied Probability. New York: Chapman & Hall; 1993.

[31] Cohen J. Statistical Power Analysis for the Behavioral Sciences. 2nd ed. Hillsdale, NJ: Lawrence Erlbaum Associates; 1988.

[32] Wu G, Liu W, Hitt J, Millon D. Spatial, temporal and muscle action patterns of Tai Chi gait. Journal of Electromyography and Kinesiology. 2004;14(3):343–354. https://doi.org/10.1016/j.jelekin.2003.09.002.

[33] Wu G, Millon D. Joint kinetics during Tai Chi gait and normal walking gait in young and elderly Tai Chi Chuan practitioners. Clinical Biomechanics. 2008;23(6):787–795. https://doi.org/10.1016/j.clinbiomech.2008.02.001.

[34] Law NY, Li JX. Biomechanics analysis of seven Tai Chi movements. Sports Medicine and Health Science. 2022;4(4):245–252. https://doi.org/10.1016/j.smhs.2022.06.002.

[35] Astephen JL, Deluzio KJ, Caldwell GE, Dunbar MJ, Hubley-Kozey CL. Gait and neuromuscular pattern changes are associated with differences in knee osteoarthritis severity levels. Journal of Biomechanics. 2008;41(4):868–876. https://doi.org/10.1016/j.jbiomech.2007.10.016.

[36] Bennell KL, Hunt MA, Wrigley TV, Hunter DJ, McManus FJ, Hodges PW, et al. Hip strengthening reduces symptoms but not knee load in people with medial knee osteoarthritis and varus malalignment: a randomised controlled trial. Osteoarthritis and Cartilage. 2010;18(5):621–628. https://doi.org/10.1016/j.joca.2010.01.010.

[37] Bennell KL, Kyriakides M, Metcalf B, Egerton T, Wrigley TV, Hodges PW, et al. Neuromuscular versus quadriceps strengthening exercise in patients with medial knee osteoarthritis and varus malalignment: a randomized controlled trial. Arthritis & Rheumatology. 2014;66(4):950–959. https://doi.org/10.1002/art.38317.

[38] Rashid SA, Hussain ME, Bhati P, Veqar Z, Parveen A, Amin I, et al. Muscle activation patterns around knee following neuromuscular training in patients with knee osteoarthritis: secondary analysis of a randomized clinical trial. Archives of Physiotherapy. 2022;12(1):19. https://doi.org/10.1186/s40945-022-00140-7.

[39] Wang C, Schmid CH, Iversen MD, Harvey WF, Fielding RA, Driban JB, et al. Comparative effectiveness of Tai Chi versus physical therapy for knee osteoarthritis: a randomized trial. Annals of Internal Medicine. 2016;165(2):77–86. https://doi.org/10.7326/M15-2143.

[40] Hunt MA, McManus FJ, Hinman RS, Bennell KL. Predictors of single-leg standing balance in individuals with medial knee osteoarthritis. Arthritis Care & Research. 2010;62(4):496–500. https://doi.org/10.1002/acr.20046.

[41] Jorge JG, Cabral ALCES, Moreira VMPS, Hattori WT, Dionisio VC. Hyperalgesia affects muscle activity and knee range of motion during a single-limb mini squat in individuals with knee osteoarthritis: a cross-sectional study. BMC Musculoskeletal Disorders. 2021;22(1):45. https://doi.org/10.1186/s12891-021-03947-w.

[42] Hug F. Can muscle coordination be precisely studied by surface electromyography? Journal of Electromyography and Kinesiology. 2011;21(1):1–12. https://doi.org/10.1016/j.jelekin.2010.08.009.

[43] Tresch MC, Jarc A. The case for and against muscle synergies. Current Opinion in Neurobiology. 2009;19(6):601–607. https://doi.org/10.1016/j.conb.2009.09.002.

Supplementary Files

This is a list of supplementary files associated with this preprint. Click to download.

- Additionalfile1.pdf
- SupplementaryTables.xlsx